J|A|C|S
ARTICLES
Published on Web 04/20/2005

# Simulations on the Thermal Decomposition of a Poly(dimethylsiloxane) Polymer Using the ReaxFF Reactive Force Field

Kimberly Chenoweth,[†] Sam Cheung,[†] Adri C. T. van Duin,[†] William A. Goddard III,*[,†] and Edward M. Kober[‡]

*Contribution from the Materials and Process Simulation Center, Division of Chemistry and Chemical Engineering, California Institute of Technology, Pasadena, California 91125, and Los Alamos National Laboratory, Los Alamos, New Mexico 87545*

Received February 15, 2005; E-mail: wag@wag.caltech.edu

***Abstract:*** To investigate the failure of the poly(dimethylsiloxane) polymer (PDMS) at high temperatures and pressures and in the presence of various additives, we have expanded the ReaxFF reactive force field to describe carbon−silicon systems. From molecular dynamics (MD) simulations using ReaxFF we find initial thermal decomposition products of PDMS to be $CH_3$ radical and the associated polymer radical, indicating that decomposition and subsequent cross-linking of the polymer is initiated by Si−C bond cleavage, in agreement with experimental observations. Secondary reactions involving these $CH_3$ radicals lead primarily to formation of methane. We studied temperature and pressure dependence of PDMS decomposition by following the rate of production of methane in the ReaxFF MD simulations. We tracked the temperature dependency of the methane production to extract Arrhenius parameters for the failure modes of PDMS. Furthermore, we found that at increased pressures the rate of PDMS decomposition drops considerably, leading to the formation of fewer $CH_3$ radicals and methane molecules. Finally, we studied the influence of various additives on PDMS stability. We found that the addition of water or a $SiO_2$ slab has no direct effect on the short-term stability of PDMS, but addition of reactive species such as ozone leads to significantly lower PDMS decomposition temperature. The addition of nitrogen monoxide does not significantly alter the degradation temperature but does retard the initial production of methane and $C_2$ hydrocarbons until the nitrogen monoxide is depleted. These results, and their good agreement with available experimental data, demonstrate that ReaxFF provides a useful computational tool for studying the chemical stability of polymers.

## Introduction

Poly(dimethylsiloxane) (PDMS; formula $-O-Si(CH_3)_2-$) is the most commonly used silicone polymer. The molecule's flexible backbone results in a high degree of mobility and consequently a low glass transition temperature. These features, combined with its high thermal stability, make PDMS useful for a broad range of applications. These applications include use in medical devices and in the automotive and electronic industries as fluids, foam cushions, lubricants, and adhesives.[1] Since PDMS is often used in high-temperature, high-pressure environments, it is important to obtain information about decomposition processes that the material may undergo in these environments; however, these harsh conditions make experimental observations challenging.

Thermal degradation of PDMS can occur by two separate mechanisms that are determined by the temperature and the heating rate of the material. When PDMS is exposed to low temperatures (753−900 K) and a slow rate of heating, the degradation has been shown to proceed via depolymerization of the polysiloxane backbone leading to formation of cyclosiloxanes.[2−5] The activation energy for this thermal depolymerization process of PDMS was determined to be 43 kcal/mol by Thomas and Kendrick.[2] Studies have proposed that the formation of the cyclic oligomers occurs via an intramolecular, cyclic, four-centered transition state where the energy for siloxane bond reorganization is lowered relative to direct Si−O bond cleavage.[2−4] The degradation of PDMS is affected by many factors, including end-group functionality,[6,7] impurities or solvent,[8] and oxidation.[8−10] In each case, these factors enhance the rate of degradation. $SiO_2$ fillers used with PDMS have been

[†] California Institute of Technology.
[‡] Los Alamos National Laboratory.

(1) Butts, M.; Cella, J.; Wood, C. D.; Gillette, G.; Kerboua, R.; Leman, J.; Lewis, L.; Rajaraman, S.; Rubinsztajn, S.; Schattenmann, F.; Stein, J.; Wengrovius, J.; Wicht, D. Silicones. In *Encyclopedia of Polymer Science and Technology*, 2nd ed.; Wiley & Sons: New York, 2003.
(2) Thomas, T. H.; Kendrick, T. C. *J. Polym. Sci., Part A-2* **1969**, *7*, 537.
(3) Thomas, T. H.; Kendrick, T. C. *J. Polym. Sci., Part A-2* **1970**, *8*, 1823.
(4) Camino, G.; Lomakin, S. M.; Lazzari, M. *Polymer* **2001**, *42*, 2395.
(5) Camino, G.; Lomakin, S. M.; Lageard, M. *Polymer* **2002**, *43*, 2011.
(6) Kang, D. W.; Rajendran, G. P.; Zeldin, M. *J. Polym. Sci., Part A: Polym. Chem.* **1986**, *24*, 1085.
(7) Deshpande, G.; Rezac, M. E. *Polym. Degrad. Stab.* **2002**, *76*, 17.
(8) Valles, E.; Sarmoria, C.; Villar, M.; Lazzari, M.; Chiantore, O. *Polym. Degrad. Stab.* **2000**, *69*, 67.
(9) Chaudry, A. N.; Billingham, N. C. *Polym. Degrad. Stab.* **2001**, *73*, 505.
(10) Grassie, N.; Macfarlane, I. G. *Eur. Polym. J.* **1978**, *14*, 875.


**10.1021/ja050980t CCC: $30.25** **© 2005 American Chemical Society**

shown to slightly enhance the thermal stability of PDMS, whereas phosphorus-containing silica lowers the onset temperature for degradation for PDMS monolayers.[11]

At higher temperatures (above 900 K) and a fast heating rate, the degradation of the PDMS occurs through a radical mechanism involving $Si-CH_3$ homolytic bond cleavage followed by hydrogen abstraction to form methane.[5,12] In the IR laser-induced degradation experiments on hexamethyldisiloxane (HMDS) and PDMS, Manders and Bellama[12] also observed the formation of ethane resulting from the combination of two methyl radicals as well as the formation of ethylene and hydrogen resulting from decomposition of ethane. The degradation of PDMS observed at high temperatures follows the thermodynamically favored pathway resulting from cleavage of the Si−C bond, which is less stable than the Si−O and C−H bonds in PDMS.

Computational methods provide an opportunity to study the decomposition of PDMS at an atomistic scale without the experimental challenges of preparing a pure sample and the interference caused by surfaces or impurities that might prematurely initiate degradation. Although the relatively large size of these polymer systems makes the study by ab initio methods computationally prohibitive, molecular dynamic methods are in principle well-suited to explore the high-temperature chemical processes in these materials. Since the conventional empirical force fields used by standard molecular dynamics programs employ rigid connectivity and cannot describe the complicated chemistry of real polymer materials, we will use a reactive force field, ReaxFF, to examine the decomposition process in PDMS.

ReaxFF[13] divides the overall system energy into various partial energy contributions as shown in eq 1.

$$E_{\text{system}} = E_{\text{bond}} + E_{\text{vdWaals}} + E_{\text{Coloumb}} + E_{\text{val}} + E_{\text{tors}} + E_{\text{over}} + E_{\text{under}} \quad (1)$$

ReaxFF allows for accurate description of bond breaking and bond formation because it is based on a bond order/bond distance relationship previously employed by Tersoff[14] and Brenner.[15] This relationship allows for a smooth transition from nonbonded to bonded systems. Since the bond orders are updated at every iteration, the connectivity of the system can continuously change. The connectivity-dependent interactions such as valence angles and torsion angles are also bond order-dependent so that their energy contributions disappear upon bond dissociation. ReaxFF incorporates nonbonded (van der Waals and Coulombic) interactions between every atom pair regardless of connectivity, and the repulsion of atoms at close range are avoided by shielding. The EEM method,[16] a geometry-dependent charge calculation scheme, is employed to account for polarization effects. One important goal in the development of ReaxFF is to obtain a transferable potential that can not only determine equilibrium bond lengths, valence angles, and so forth from the chemical environment of the system but also handle coordination changes associated with reactions.

ReaxFF has been successfully used to simulate various materials, including hydrocarbons,[13] nitramines,[17] aluminum/aluminum oxides,[18] and silicon/silicon oxides.[19] To study the high-temperature thermal properties of PDMS, the ReaxFF description of Si/SiO materials has been extended to include silicon−carbon systems. Using ReaxFF, we can simulate changes in bonding associated with the degradation of a material and observe the distribution of products formed, gaining insight into how decomposition initiates and proceeds. By performing ReaxFF simulations at different temperatures, we can determine the temperature-dependent reaction rates, allowing us to directly calculate Arrhenius parameters for PDMS decomposition. We also examine the effects of additives such as water, silicon oxide, ozone, and nitrogen monoxide on PDMS decomposition.

## Computational Methods

**Quantum Chemical Calculations.** The force field was constructed by adding quantum chemical (QC) data for systems relevant to PDMS chemistry to the ReaxFF training set for Si/SiO materials.[19] QC data for nonperiodic systems was obtained from DFT calculations performed using Jaguar (version 5.5)[20] using the B3LYP functional[21] and Pople's 6-311G**++ basis set.[22] The Mulliken charges were obtain using Pople's 6-31G** basis set.[23] To obtain the equation of state for disiloxane diol $(HOMe_2Si)_2O$ crystal, DFT calculations were performed with the plane-wave code CASTEP[24] (version 3.8) module in Cerius$^2$.[25] The generalized gradient approximation (GGA) proposed by Perdew, Burke, and Ernzerhof[26] was used for the exchange-correlation energy, and ultrasoft pseudopotentials were used to replace the core electrons. We used the Perdew−Wang implementation of GGA[27] with a kinetic energy cutoff of 380 eV. The Monkhorst−Pack scheme[28] was used to generate the *k*-space grid with a 0.1 $Å^{-1}$ spacing.

**Molecular Dynamics Simulations.** Simulations were performed on pure PDMS systems as well as PDMS in the presence of various additives. The pure PDMS polymer consisted of eight linear polymer strands per unit cell (each strand consists of 12 monomer units) at an initial density of 1.227 g/cm$^3$. Four other densities of the polymer were also studied, including 0.974, 1.022, 1.534, and 1.753 g/cm$^3$. These structures were obtained by cubic expansion or compression of the original system. Simulations were also performed on PDMS polymer with a 10% water content (32 water molecules) and PDMS in contact with an amorphous $SiO_2$ slab, 20 ozone molecules, and 20 NO molecules.

The procedure used for simulation of the polymer involved minimization of each structure using low-temperature MD. Next, all structures were equilibrated at 2500 K using NVT-MD simulation (using a Berendsen thermostat[29]) and a time step of 0.05 fs with the following

(11) (a) Kumudinie, C.; Mark, J. E. *Mater. Res. Soc. Symp. Proc.* **1999**, *576*, 331. (b) Bogatyr'ov, V. M.; Borysenko, M. V. *J. Therm. Anal. Calorim.* **2000**, *62*, 335.
(12) Manders, W. F.; Bellama, J. M. *J. Polym. Sci., Part A: Polym. Chem.* **1985**, *23*, 351.
(13) van Duin, A. C. T.; Dasgupta, S.; Lorant, F.; Goddard, W. A., III. *J. Phys. Chem. A* **2001**, *105*, 9396.
(14) Tersoff, J. *Phys. Rev. B* **1988**, *37*, 6991.
(15) Brenner, D. W. *Phys. Rev. B* **1990**, *42*, 9458.
(16) Mortier, W. J.; Ghosh, S. K.; Shankar, S. J. *J. Am. Chem. Soc.* **1998**, *120*, 2641.
(17) Strachan, A.; van Duin, A. C. T.; Chakraborty, D.; Dasgupta, S.; Goddard, W. A., III. *Phys. Rev. Lett.* **2003**, *91*, 098301.
(18) Zhang, Q.; Cagin, T.; van Duin, A.; Goddard, W. A., III.; Qi, Y.; Hector, L. G., Jr. *Phys. Rev. B* **2004**, *69*, 045423.
(19) van Duin, A. C. T.; Strachan, A.; Stewman, S.; Zhang, Q.; Xu, X.; Goddard, W. A., III. *J. Phys. Chem. A* **2003**, *107*, 3803.
(20) *Jaguar 5.5*; Schrodinger, LLC: Portland, OR, 2003.
(21) (a) Becke, A. D. *J. Chem. Phys.* **1993**, *98*, 5648. (b) Lee, C.; Yang, W.; Parr, R. G. *Phys. Rev. B* **1988**, *37*, 785.
(22) (a) Krishnan, R.; Binkley, J. S.; Seeger, R.; Pople, J. A. *J. Chem. Phys.* **1980**, *72*, 650. (b) Clark, T.; Chandrasekhar, J.; Schleyer, P. V. R. *J. Comput. Chem.* **1983**, *4*, 294.
(23) (a) Hariharan, P. C.; Pople, J. A. *Theor. Chim. Acta* **1973**, *28*, 213. (b) Francl, M. M.; Petro, W. J.; Hehre, W. J.; Binkley, J. S.; Gordon, M. S.; Frees, D. J.; Pople, J. A. *J. Chem. Phys.* **1982**, *77*, 3654.
(24) Payne, M. C.; Teter, M. P.; Allan, D. C.; Arias, T. A.; Joannopoulos, J. D. *Rev. Mod. Phys.* **1992**, *64*, 1045.
(25) *Cerius*$^2$, version 4.0; Accelrys: San Diego, CA, 1999.
(26) Perdew, J. P.; Burke, K.; Ernzerhof, M. *Phys. Rev. Lett.* **1996**, *77*, 3865.
(27) Perdew, J. P.; Wang, Y. *Phys. Rev. B* **1992**, *46*, 6671.
(28) Monkhorst, H. J.; Pack, J. D. *Phys. Rev. B* **1976**, *13*, 5188.

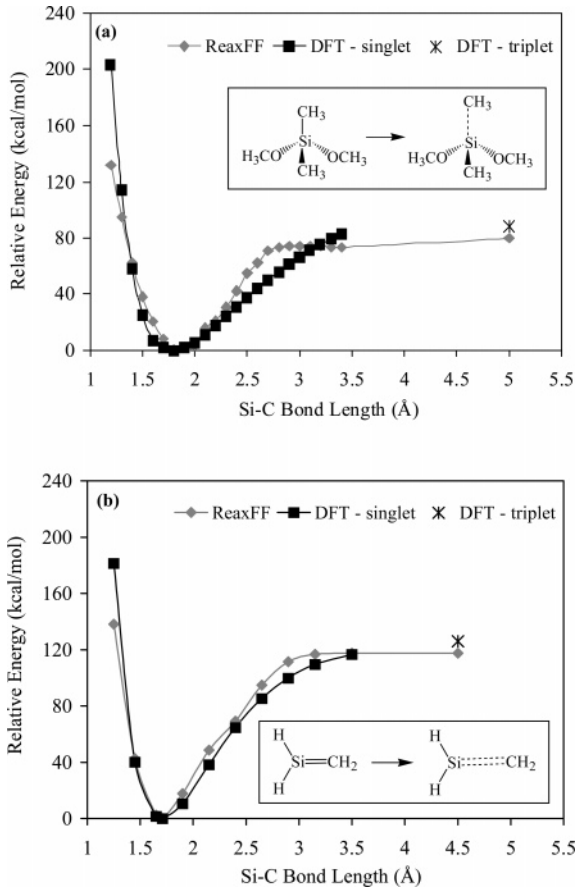


***Figure 1.*** Comparison of ReaxFF and QC energies for Si−C single (a) and double (b) bond dissociations.

exceptions: PDMS in contact with ozone and PDMS in contact with NO were equilibrated at 1000 K using a time step of 0.1 fs. The equilibrated structures were then used in the cookoff simulation where the temperature was at a rate of 266 K/ps for 7.5 ps. The cookoff simulations for the PDMS in contact with ozone was 5 ps in length, and PDMS in contact with NO was 12.5 ps in length with the same rate of temperature change, 266 K/ps. The bond order cutoff for molecule recognition used in the analysis for all systems was 0.3 Å.

## Results and Discussion

**ReaxFF Force Field Optimization.** The ReaxFF parameters were determined by combining the Si/SiO training set with the results from QC calculations for systems related to PDMS chemistry; these parameters are available in the Supporting Information. The results of fitting with respect to the original Si/SiO training set are consistent with those published earlier,[19] and only the results for the systems relevant to PDMS chemistry are presented here. One goal of ReaxFF development is to obtain parameters that are transferable. Since the complete training set contains both the Si/SiO training set in addition to the new data relevant to PDMS, the resulting force field is general and capable of describing other systems containing Si, O, C, and H.

To optimize the silicon−carbon bond energy, we used the dissociation pathway for the Si−C single bond in $Si(CH_3)_2(OCH_3)_2$ (Figure 1a) and $H_3Si-CH_3$ and the Si═C double bond in $H_2Si{=}CH_2$ (Figure 1b). To optimize the ReaxFF parameters, the DFT results for the singlet case were used around the equilibrium bond distance while the dissociation limit was fitted against the DFT results for the triplet state. The Si−C bond parameters are given in Table 1.

***Table 1.*** ReaxFF Silicon−Carbon Bond Parameters

| | |
|---|---|
| **Bond Radius and van der Waals Parameters** | |
| $r^{\alpha}$ (Å) | 1.75 |
| $r^{\pi}$ (Å) | 1.51 |
| $r_{vdw}$ (Å) | 2.06 |
| ee (kcal/mol) | 0.05 |
| aa | 13.23 |
| **Bond Energy Parameters** | |
| $D_e^{\alpha}$ (kcal/mol) | 119.16 |
| $D_e^{\pi}$ (kcal/mol) | 83.35 |
| $p_{be,1}$ | 0.12 |
| $p_{be,2}$ | 0.25 |
| $p_{be,3}$ | 0.10 |
| **Bond Order Parameters** | |
| $p_{bo,1}$ | −0.11 |
| $p_{bo,2}$ | 6.50 |

***Table 2.*** ReaxFF Valence Angle Parameters

| | $\Theta_{0,0}$ (degree) | $k_a$ (kcal/mol) | $k_b$ (kcal/mol) | $p_{v,1}$ | $p_{v,2}$ |
|---|---|---|---|---|---|
| C−C−Si | 64.56 | 20.95 | 1.98 | 1.04 | 1.05 |
| C−Si−C | 69.61 | 20.49 | 2.14 | 1.04 | 1.13 |
| Si−Si−C | 71.36 | 20.35 | 2.04 | 1.01 | 1.02 |
| Si−C−Si | 58.76 | 16.69 | 1.99 | 0.99 | 1.01 |
| Si−C−H | 67.26 | 11.85 | 2.42 | 1.02 | 1.02 |
| C−Si−H | 71.05 | 15.31 | 2.41 | 1.05 | 1.13 |
| Si−O−C | 83.45 | 13.30 | 0.92 | 0.97 | 1.28 |
| C−Si−O | 60.18 | 41.22 | 1.36 | 1.03 | 1.01 |
| O−C−Si | 76.61 | 5.48 | 0.99 | 0.98 | 1.28 |

The valence angle parameters were optimized to represent angle bending energies from DFT calculations on various clusters and are given in Table 2. For silicon−carbon systems, there are nine valence angles that need to be represented. These include C−C−Si, C−Si−C, Si−Si−C, Si−C−Si, Si−C−H, C−Si−H, O−C−Si, Si−O−C, and C−Si−O. For each angle, the geometry of the representative molecule was optimized with the angles of interest fixed to obtain angle bending energies relative to the optimal geometry. The results from DFT and ReaxFF for Si−O−C and C−Si−O are shown in Figure 2. The PDMS dimer ($CH_3O-Si(CH_3)_2-O-Si(CH_3)_2-OCH_3$) was used as the representative molecule for both valence angles. The results for the remaining angles and Si−C bond have been supplied in the Supporting Information.

In ReaxFF, the charge distributions are calculated using the EEM method.[16] The Mulliken charge distributions obtained from DFT calculations were used to optimize the EEM charge parameters. The partial charges from DFT and ReaxFF for the atoms of $Si(CH_3)_2(OCH_3)_2$, $Si(CH_3)_2(OH)_2$, *c*-$(Si(CH_3)_2-O)_3$ (six-membered ring), $HO-Si(CH_3)_2-O-Si(CH_3)_2-OH$ (disiloxane diol), and the PDMS dimer are given in Figure 3.

To sample possible reactions in Si−C systems relating to the decomposition of PDMS, DFT and ReaxFF reaction energies were obtained and are reported in Table 3. These reactions include not only energetically favorable clusters but also strained and energetically less favorable clusters that test the ability of ReaxFF to represent both cases. Cleavage of the Si−O bond is important in the degradation process for silicones exposed to water, and the DFT barriers calculated by Cypryk and Apeloig[30]

(29) Berendsen, H. J. C.; Postma, J. P. M. van Gunsteren, W. F.; DiNola, A.; Haak, J. R. *J. Chem. Phys.* **1984**, *81*, 3684

(30) Cypryk, M.; Apeloig, Y. *Organometallics* **2002**, *21*, 2165.

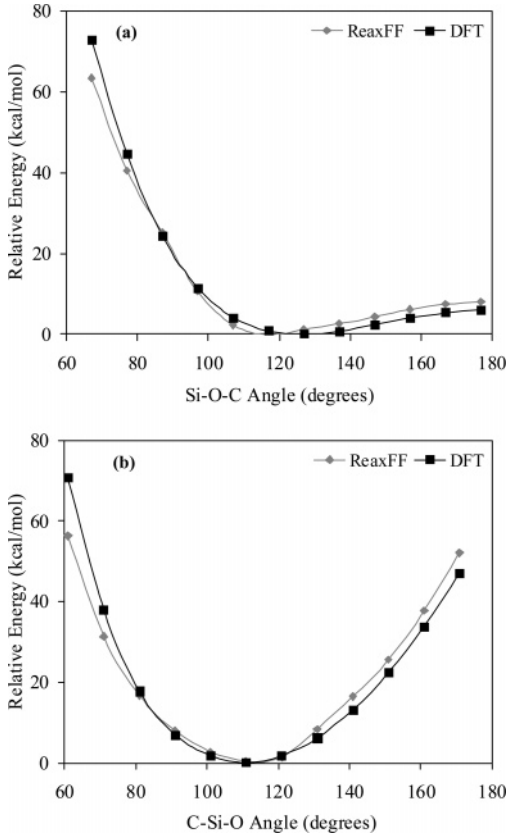


***Figure 2.*** ReaxFF and QC distortion energies for the Si−O−C (a) and C−Si−O (b) angles in a PDMS dimer.

for hydrolysis of the siloxane bond under neutral conditions were added to the training set. The ReaxFF and DFT energies for these systems are reported in Table 4.

A key application of ReaxFF is the simulations of condensed phase PDMS systems, particularly at high pressure and high temperature. A compression/expansion curve was obtained for disiloxane diol, which has a well-defined crystal structure.[31] The ability of ReaxFF to represent the equation of state of the disiloxane diol crystal is shown in Figure 4. Since a SiC condensed phase is a potential product from the decomposition of PDMS, the stability of the SiC (diamond phase) relative to that of C (diamond phase) and α-Si (diamond phase) was obtained from ReaxFF (−14.8 kcal/mol) and DFT methods (−15.0 kcal/mol). The Crystal Builder module in Cerius[2] and the unit cell parameters reported by Albouy[32] were used to construct the PDMS crystal. Optimization of the PDMS crystal with ReaxFF gave a density of 1.095 g/cm$^3$, which is 7% smaller than the experimental density of 1.180 g/cm$^3$ (measured at 59 K).[32]

**Cookoff Simulation.** A cookoff simulation of the PDMS polymer was performed to obtain an overview of the decomposition process. Using a heating rate of 266 K/ps, we find that degradation of the PDMS polymer initiates at about 2800 K. Figure 5 shows the time evolution of the production of various compounds from the decomposition of the polymer. The density of the polymer used in the simulation is 1.227 g/cm$^3$, and the pressure change observed during the simulation was 7.15 GPa (Table 5). At these high temperatures, the polymer strands are very mobile and are continuously forming and breaking bonds with neighboring strands before initiation of decomposition. Therefore, the total number of polymer strands observed is less than eight; cross-linked strands are accounted for as "others". We observe an oscillation between the number of original polymer strands and the number of "others" until the degradation process is initiated. The first products observed in the cookoff simulation are the $CH_3$ radical and the resulting polymer radical. The silicon−carbon bond is 30 kcal/mol weaker than a siloxane bond. Therefore, cleavage of the Si−C bond initiates the decomposition process; this is consistent with experimental results.[5,12] A secondary reaction involving the abstraction of a hydrogen by the $CH_3$ radicals leads to the formation of methane, the main degradation product. Various $C_2$ hydrocarbons including $C_2H_5$ radical, $C_2H_4$, $C_2H_3$ radical, and $C_2H_2$ as well as molecular hydrogen are first observed after 4.5 ps and are consistent with the decomposition of ethane and ethylene as described by Manders and Bellama.[12] To analyze the final state of the decomposed material, the molecular weight distribution of the silicon−carbon-containing systems in the final configuration was determined and is shown in Figure 6. The final material is enriched in silicon oxide compared to the bulk material due to a 29.2% loss of carbon and a 32.5% loss of hydrogen. The final configuration of the polymer material consists of several small fragments of less than 310 amu and one large fragment with a mass of 5695 amu.

**Temperature-Dependent PDMS-Decomposition.** To analyze the kinetics and the details of the decomposition process, a series of 12 NVT-MD simulations were performed with a time step of 0.05 fs lasting 20 ps for temperatures of 2400−3500 K at 100 K intervals. Table 6 shows a detailed analysis of the composition of the methane molecules produced in the 2400, 2700, and 3000 K NVT-MD simulations. At 2400 K, we find

***Table 3.*** Comparison of DFT and ReaxFF Reaction Energies (in kcal/mol)

| reaction | *E* (DFT) | *E* (ReaxFF) |
|---|---|---|
| $Si(OH)_4 \rightarrow SiO_2 + 2\ H_2O$ | 127 | 137 |
| dissociation of $CH_4$ from *c*-$(Si(CH_3)_2{-}O)_3$ | 55 | 51 |
| dissociation of $CH_3CH_3$ from *c*-$(Si(CH_3)_2{-}O)_3$ | 38 | 72 |
| $Si(OH)_2(CH_3)_2 \rightarrow SiO_2 + 2\ CH_4$ | 76 | 88 |
| $Si(OCH_3)_2(CH_3)_2 \rightarrow SiO_2 + 2\ CH_3CH_3$ | 51 | 76 |
| $Si(OCH_3)_2(CH_3)_2 + 2\ H_2 \rightarrow SiO_2 + 4\ CH_4$ | 3 | 10 |
| $Si(OCH_3)_2(CH_3)_2 + 2\ H_2 \rightarrow$ *c*-$(O{-}O{-}Si(CH_3)_2) + 2\ CH_4$ | 29 | 20 |
| $Si(OCH_3)_2(CH_3)_2 \rightarrow$ *c*-$(O{-}O{-}Si(CH_3)_2) + CH_3CH_3$ | 77 | 57 |
| PDMS dimer $+ H_2 \rightarrow {}^1/_2\ SiO_2 + {}^7/_2\ CH_4 + CO_2 + {}^1/_2$ *c*-$(H_2Si{-}CH_2)_3$ | 80 | 106 |
| PDMS dimer $+ 2\ H_2 \rightarrow CO_2 + 3\ CH_4 + H_2O + {}^2/_3$ *c*-$(H_2Si{-}CH_2)_3$ | 57 | 85 |
| $HO{-}Si(CH_3)_2{-}O{-}Si(CH_3)_2{-}O \rightarrow {}^1/_2\ SiO_2 + {}^3/_2\ CH_4 + CO_2 + H_2 + {}^1/_2$ *c*-$(H_2Si{-}CH_2)_3$ | 142 | 154 |
| $HO{-}Si(CH_3)_2{-}O{-}Si(CH_3)_2{-}O \rightarrow CO_2 + CH_4 + H_2O + {}^2/_3$ *c*-$(H_2Si{-}CH_2)_3$ | 119 | 135 |

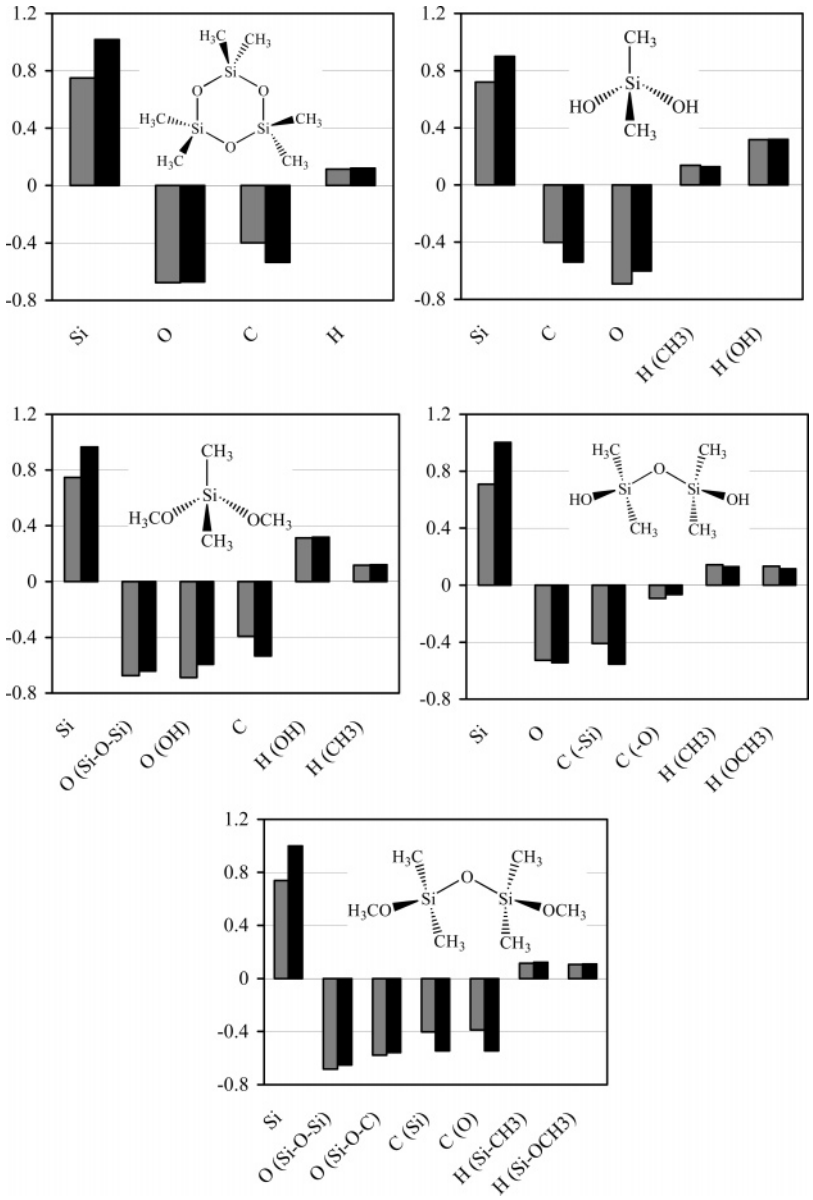


***Figure 3.*** Comparison between Mulliken charge distributions obtained from DFT (black) and charge distributions obtained from ReaxFF (gray). The notes in parentheses define the environment of the atoms.

***Table 4.*** Relative Energies[a] (kcal/mol) for Hydrolysis of Disiloxane and Disiloxanol by Water Clusters $(H_2O)_n$ ($n$ = 1, 2, 4)

| | DFT [30] | | ReaxFF | |
|---|---|---|---|---|
| $n$ | products | TS | products | intermediate |
| | Disiloxane + $(H_2O)_n \rightarrow 2\ H_3SiOH + (H_2O)_{n-1}$ | | | |
| 1 | −0.2 | −33.9 | −1.7 | −37.3 |
| 2 | −0.2 | −24.7 | −1.9 | −17.9 |
| 4 | −1.2 | −23.0 | 2.5 | −12.6 |
| | Disiloxanol + $(H_2O)_n \rightarrow H_3SiOH + H_2Si(OH)_2 + (H_2O)_{n-1}$ | | | |
| 1 | 0.0 | −31.9 | 1.8 | −32.2 |
| 4 | −8.2 | −17.5 | −9.8 | −22.5 |

[a] The energies shown are relative to the energy of the reactant for each reaction.

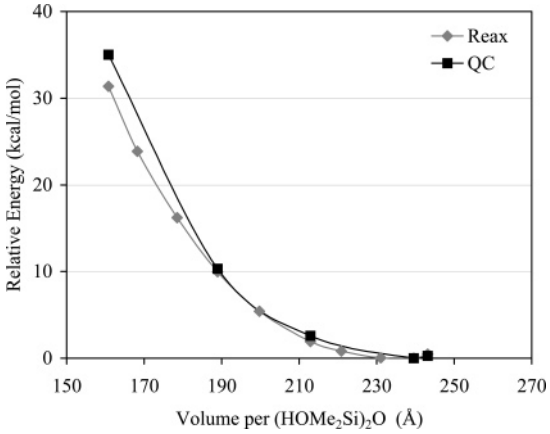


***Figure 4.*** ReaxFF and QC equations of state (compression and expansion) for the disiloxane diol crystal, $(HOMe_2Si)_2O$.

that the methane molecules formed contain all of the hydrogen atoms originally bound to the carbon in the methyl group. Five of the methane molecules formed in the 60 ps NVT-MD simulation at 2400 K came from a methyl radical that abstracted a hydrogen from a methyl group on an adjacent polymer strand,

(31) Polishchuk, A. P.; Timofeeva, T. V.; Antipin, M. Y.; Makarova, N. N.; Golovina, N. A.; Struchkov, Y. T.; Lavrentovich, O. D. *Organomet. Chem. USSR* **1991**, *4*, 147.

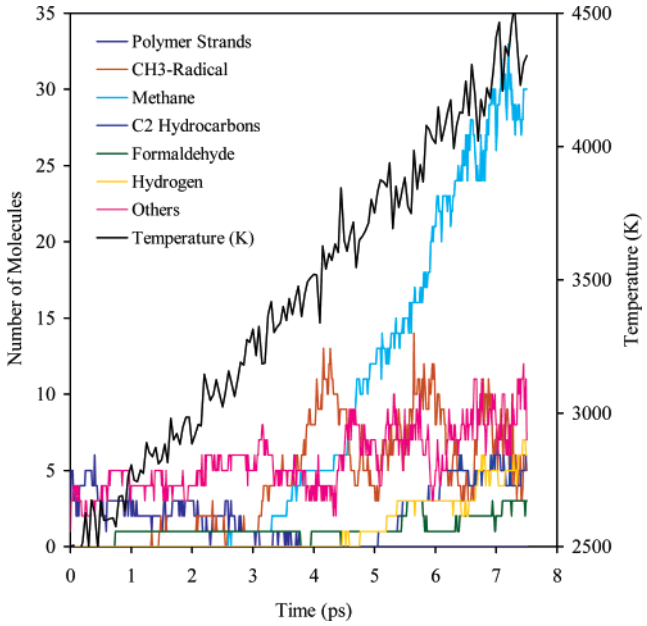


***Figure 5.*** Time evolution of the compounds observed during cookoff simulation of eight PDMS polymer strands at a density of 1.227 g/cm$^3$.

***Table 5.*** Pressure of the Initial and Final Configuration of Each System for the Cookoff Simulations

| | pressure (GPa) | |
|---|---|---|
| | initial configuration | final configuration |
| Pure PDMS | | |
| PDMS (0.974 g/cm$^3$) | 2.34 | 7.17 |
| PDMS (1.022 g/cm$^3$) | 3.81 | 7.79 |
| PDMS (1.227 g/cm$^3$) | 4.05 | 11.20 |
| PDMS (1.534 g/cm$^3$) | 8.63 | 17.96 |
| PDMS (1.753 g/cm$^3$) | 12.24 | 27.11 |
| PDMS with Additives | | |
| PDMS/$H_2O$ | 7.05 | 12.96 |
| PDMS/$SiO_2$ | 2.98 | 7.52 |
| PDMS/$O_3$ | 1.03 | 2.36 |
| PDMS/NO | 1.34 | 5.50 |

and there is only one case in which the methyl radical abstracts a hydrogen from a methyl group on the same strand. As the temperature and duration of the simulation increase, there is a decrease in the amount of methane molecules where the carbon atom retains its original hydrogen atoms. This is probably related to the increase in the concentration of radicals in the system at elevated temperatures as these attack the stable molecules and facilitate hydrogen exchange. A population analysis of the types

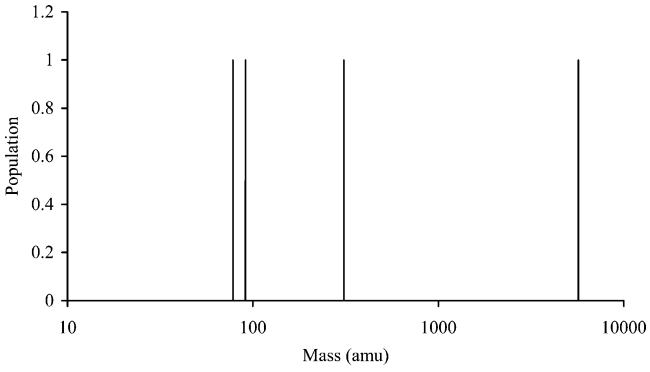


***Figure 6.*** Mass spectrum corresponding to the silicon-containing molecules in the final configuration of PDMS (density = 1.227 g/cm$^3$). The mass of one PDMS polymer strand is 889.25 amu.

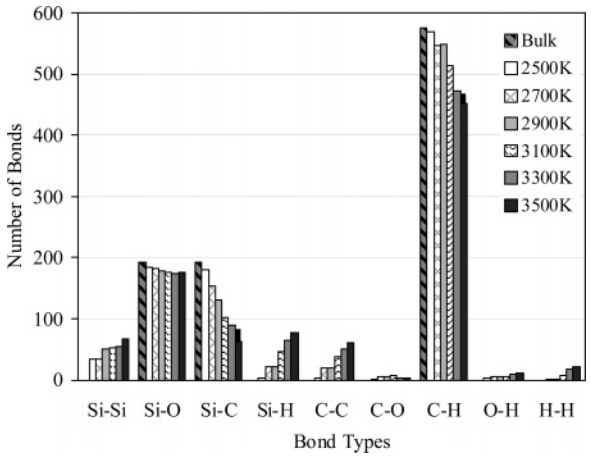


***Figure 7.*** Population of bond types in final configuration from the NVT-MD simulations. The values for bulk PDMS before the simulation are given as a reference.

of bonds observed in the final configuration at various temperatures is shown in Figure 7. At temperatures of 3000 K or less, Si−C bonds are breaking to form $CH_3$ radicals and C−H bonds are forming, resulting in methane production. There are also a small number of C−C bonds forming, resulting in the formation of $C_2$ hydrocarbons. As the temperature increases, there is an increase in the number of C−C and H−H bonds forming, resulting in an increase in the number of $C_2$ hydrocarbon and hydrogen molecules. There is also an increase in the number of Si−Si bonds forming, resulting in a more cross-linked state for the final silicon oxide rich material. There is a reduction in the silicon/carbon ratio in the bulk phase from 1:2 to 1:1.4. The 3500 K NVT-MD simulation was extended to 60 ps, and the final configuration of the system is shown in Figure 8. A complete list of the products observed in this simulation is provided in Table 7. Analysis of the structure of the large silicon-containing molecule ($C_{75}H_{216}O_{92}Si_{91}$) revealed that each oxygen atom is bound to two silicon atoms as in bulk PDMS except for eight silanol (Si−OH) groups and one of each of the following groups: C−OH, C═O, and Si−O−C. The number of silicon atoms with two methyl groups has been reduced by 88%, leaving 32.6% of the silicon atoms bonded to one carbon atom and 51.1% bonded to no carbon atoms. A total of 46.7% of the carbon atoms in this molecule are methyl groups, and the remaining ones make up larger alkyl groups. The number of silicon atoms bonded to more than two oxygen atoms has increased compared to the original polymer material.

The $CH_3$ radical is observed as an intermediate in the decomposition process and proceeds in a fast secondary reaction to form methane as the primary product. Therefore, methane is used as a guide in studying the kinetics of PDMS decomposition. Figure 9 shows the rate of methane production in the NVT-MD simulations at various temperatures. The data set used to obtain the rate ($k$) was taken from 20 ps NVT-MD simulations at 2400−3500 K. For those temperatures (3200−3500 K) that produce a high concentration of methane molecules, the data used to obtain the rate of methane production was obtained from 0 ps until the time that 30 methane molecules were produced. Otherwise, the data for methane production from the entire simulation were used.

(32) Albouy, P. A. *Polymer* **2000**, *41*, 3083.

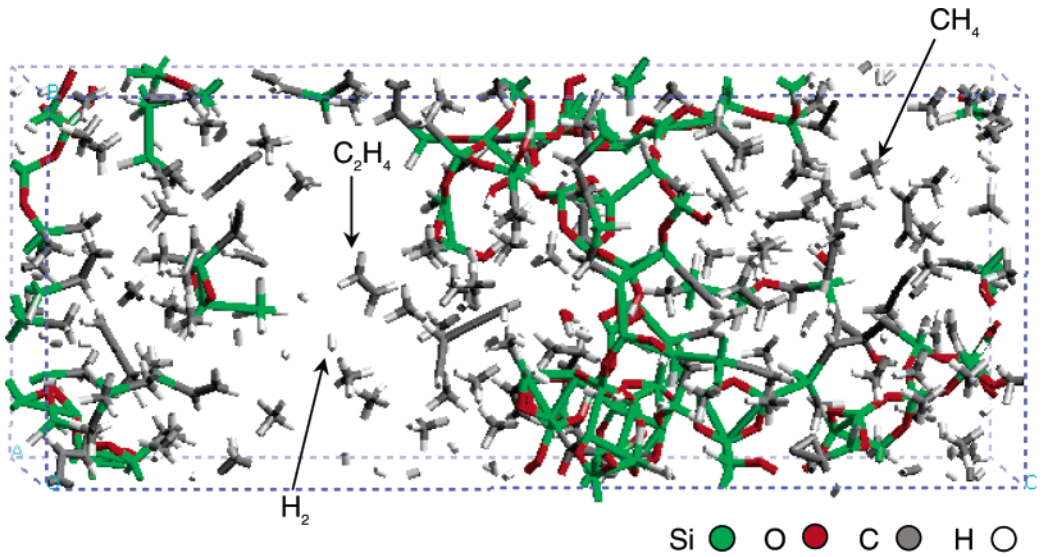


***Figure 8.*** Final configuration of the 3500 K NVT-MD simulation of PDMS at a density of 1.227 g/cm$^3$.

***Table 6.*** Percentage of Methane Molecules Observed during the Simulation that Retained at Least One, Two, or Three Hydrogen Atoms from the Original Methyl Group Prior to PDMS Degradation

| | | percentage of methane molecules with *n* original hydrogens | | | |
|---|---|---|---|---|---|
| NVT-MD simulation[a] | total methane molecules formed | *n* = 3 | *n* = 2 | *n* = 1 | *n* = 0 |
| 2400 K − 20 ps | 2 | 100 | | | |
| 2400 K − 60 ps | 6 | 100 | | | |
| 2700 K − 20 ps | 10 | 100 | | | |
| 2700 K − 60 ps | 26 | 81.8 | 13.6 | 4.6 | |
| 3000 K − 20 ps | 21 | 81 | 19 | | |
| 3000 K − 60 ps | 46 | 48.8 | 46.4 | 2.4 | 2.4 |

[a] The temperature of the NVT-MD simulation is given with the length of the simulation for which results are given.

***Table 7.*** Products Formed in 3500 K NVT-MD Simulation of PDMS (1.227 g/cm$^3$)

| number of molecules | molecular formula | molecular weight |
|---|---|---|
| 1 | $C_{75}H_{216}O_{92}Si_{91}$ | 5143.10 |
| 1 | $C_4H_7O_2Si_2$ | 143.17 |
| 1 | $C_6H_{11}Si$ | 111.15 |
| 1 | $C_3H_9Si$ | 73.13 |
| 1 | $C_5H_4$ | 64.03 |
| 1 | $C_4H_6$ | 54.05 |
| 1 | $C_3H_3$ | 39.02 |
| 1 | $C_3H$ | 37.01 |
| 1 | $H_4Si$ | 32.09 |
| 1 | $CH_2O$ | 30.02 |
| 6 | $C_2H_4$ | 28.03 |
| 2 | $C_2H_3$ | 27.02 |
| 6 | $C_2H_2$ | 26.02 |
| 1 | $C_2H$ | 25.01 |
| 1 | $C_2$ | 24.00 |
| 1 | $H_2O$ | 18.02 |
| 54 | $CH_4$ | 16.03 |
| 2 | $CH_3$ | 15.02 |
| 23 | $H_2$ | 2.02 |

The rate as a function of the number of methane molecules formed was obtained from a linear fit of the data set described above at each temperature. The rate as a function of inverse temperature is shown in the Arrhenius plot in Figure 10. To obtain an estimate of the errors associated with calculating the Arrhenius parameters from the NVT-MD simulations, two additional NVT-MD simulations with different initial configurations were performed at 2400, 2800, 3100, and 3500 K, and these data are also shown in Figure 10. The rate of methane production from trial 1 was used to calculate the Arrhenius parameters. The calculated pre-exponential or frequency factor (A) is 1.3 × 10$^{15}$ mol L$^{-1}$ s$^{-1}$, and the activation energy is 53 kcal/mol.

This activation energy is substantially lower than the Si−C bond dissociation energy in PDMS (about 85 kcal/mol), which indicates that the formation of the methyl radical is not simply a result of Si−C bond cleavage but is probably the result of a concerted reaction. One possibility of such a concerted reaction is the formation of a partial bond between two silicon atoms, resulting in an overcoordination of the silicon atoms leading to

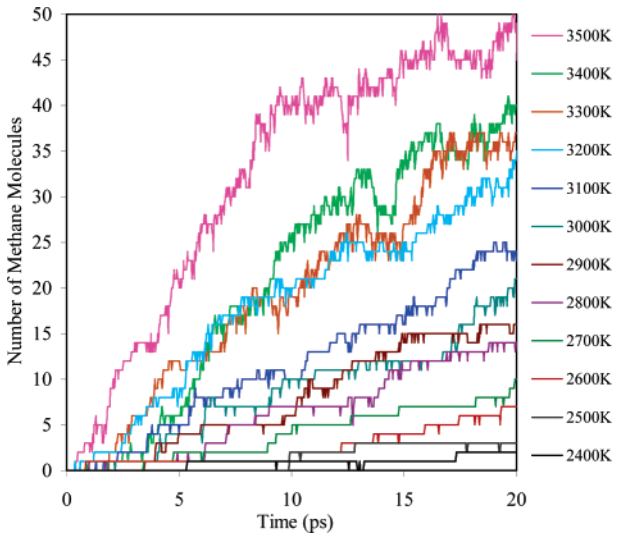


***Figure 9.*** Population of methane molecules observed in NVT-MD simulations at various temperatures.

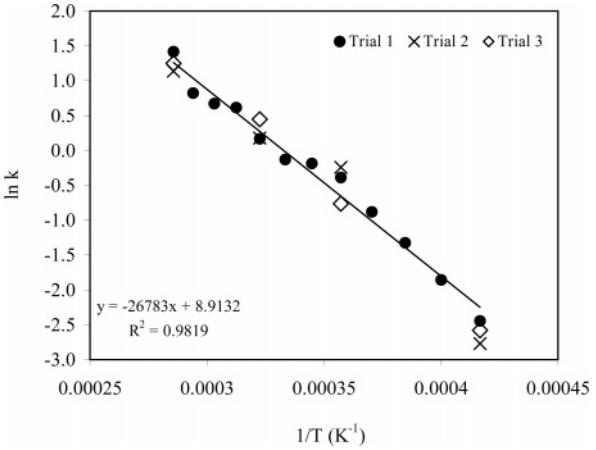


***Figure 10.*** Rate of production of methane as a function of temperature. The results from additional NVT-MD simulations with differing initial configurations are shown to provide an indication of the error. The line represents the fit of the data from trial 1 to the Arrhenius expression.

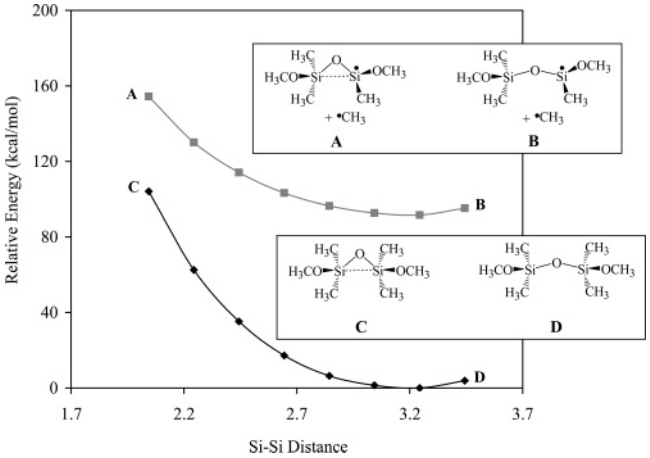


***Figure 11.*** QC energy as a function of the Si−Si bond distance in the PDMS dimer (black) and the PDMS dimer radical (gray). The difference between any two energies at a particular Si−Si distance is the energy for dissociation of the Si−C bond.

a lower energy barrier for the cleavage of a Si−C bond. To investigate this hypothesis, we used the PDMS dimer as a model for the PDMS polymer system and performed QC calculations to determine the Si−C bond dissociation energy as a function of the Si−Si bond distance. The dissociation energy is obtained from the DFT energies where the Si−Si bond was fixed at various distances for both the PDMS dimer and the PDMS dimer radical, which consists of breaking one Si−C bond from the original molecule to form a methyl radical. The results of these calculations are shown in Figure 11 and indicate that shortening of the Si−Si distance in the polymer indeed leads to a reduction of the Si−C dissociation energy. The decrease of the Si−Si bond distance in the PDMS dimer is also accompanied by a lengthening of the Si−C bonds. Therefore, vibrational excursions that reduce the Si−Si distance in the polymer would lower the activation energy for Si−C bond cleavage.

**Pressure-Dependent PDMS Decomposition.** Cookoff simulations were performed for a range of densities to investigate the effect of pressure on decomposition of PDMS. The molecular weight distribution of the resulting polymer material is given in Figure 12 at two of the five densities studied, including 0.973 g/cm$^3$ (room-temperature density of PDMS[33]) and 1.753 g/cm$^3$. The pressure of the equilibrated system and the system at the end of the cookoff simulation is given in Table 5. At lower densities, the final state of the polymer material consists of many low molecular weight fragments (Figure 12a). As the density increases, there is increased cross-linking of the resulting silicon oxide material, resulting in one high molecular weight fragment and only a few small oligomers (Figure 12b). Analysis of the types of bonds present in the final configuration from the simulations is shown in Figure 13. As the density of the PDMS increases, there is a decrease in the number of Si−C bonds cleaved as well as an observed decline in the formation of $CH_3$ radicals and an increase in the temperature for decomposition. At increased densities, the linear strands of the polymer become more tightly packed, reducing its flexibility. If the vibrational motions of the polymer are limited, the benefit of lowering the activation energy for Si−C bond cleavage through reducing the silicon−silicon distance in the polymer would be less significant. This results in an increase in the stability of the PDMS at elevated pressures.

**PDMS Decomposition in the Presence of Additives.** To investigate the effect of water on PDMS decomposition, we performed a cookoff simulation of the polymer with 10% (w/w) water content. Figure 14 shows the products observed from this simulation. Compared with the PDMS polymer, thermal decomposition of PDMS/$H_2O$ resulted in the production of more methane molecules, and a new product, methanol, was observed. The initial degradation of the polymer occurs in the same manner as pure PDMS through Si−C bond cleavage to form $CH_3$ radicals that undergo secondary reactions to form methane or methanol. PDMS is not completely stable to water, and we observe lower molecular weight polymers as a result of hydrolytic bond cleavage. Since condensation is favored at high temperatures, the low molecular weight oligomers can condense and undergo cross-linking to form larger molecular weight polymers. The competition between hydrolysis and condensation results in an overall reduction in the amount of cross-linking observed in the final decomposed material compared to that for PDMS. There are 30% more Si−C bonds cleaved than was observed for pure PDMS, and this is consistent with the increase in the number of methane molecules in addition to the methanol that was observed.

To study the effects of other additives on PDMS, we performed cookoff simulations on PDMS in contact with an amorphous $SiO_2$ slab, PDMS in contact with ozone, and PDMS in contact with NO. The initial configuration for the PDMS/$SiO_2$ system is shown in Figure 15. In comparison with pure PDMS, the degradation of PDMS/$SiO_2$ system results in production of new decomposition products, water, and a small amount of methanol (Figure 16). We observe an increase in the number of O−H bonds formed during the simulation, which is consistent with the formation of water. We also observe formation of Si−Si bonds resulting from cross-linking of the polymer yielding a final material that consists primarily of a large molecular weight material in addition to a few low molecular weight products. The stability of PDMS was not significantly affected by the presence of the silicon oxide material.

The addition of ozone to PDMS resulted in the lowering of the temperature for initiation of decomposition to 2000 K (Figure

(33) Mark, J. E. *Physical Properties of Polymers Handbook*; Woodbury: New York, 1996.

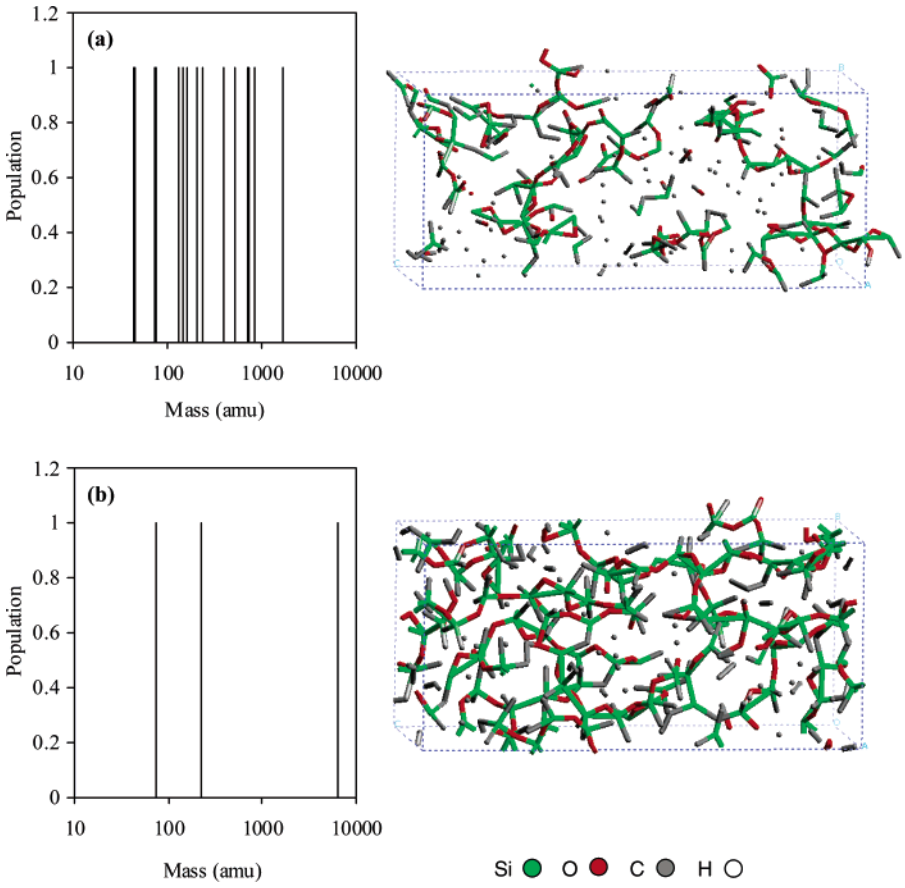


***Figure 12.*** Mass spectra and configurations corresponding to the silicon-containing molecules observed after cookoff simulations of PDMS with a density of 0.973 g/cm$^3$ (a) and 1.753 g/cm$^3$ (b). The mass of one PDMS polymer strand is 889.25 amu. The final configuration of the system at both densities is shown without hydrogens for clarity.

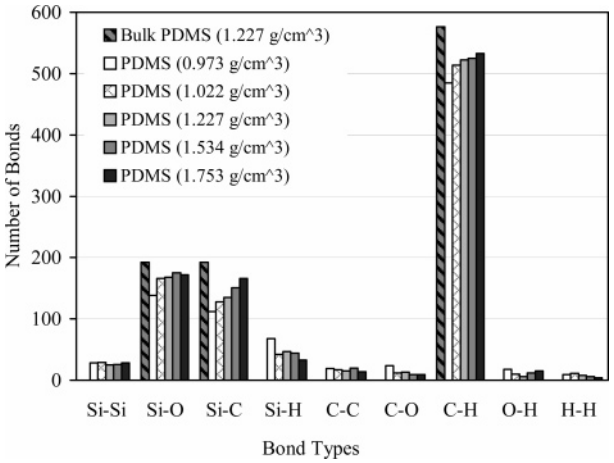


***Figure 13.*** Population of bond types in the final configuration from the cookoff simulations at different densities. The values for bulk PDMS before the simulation are given as a reference.

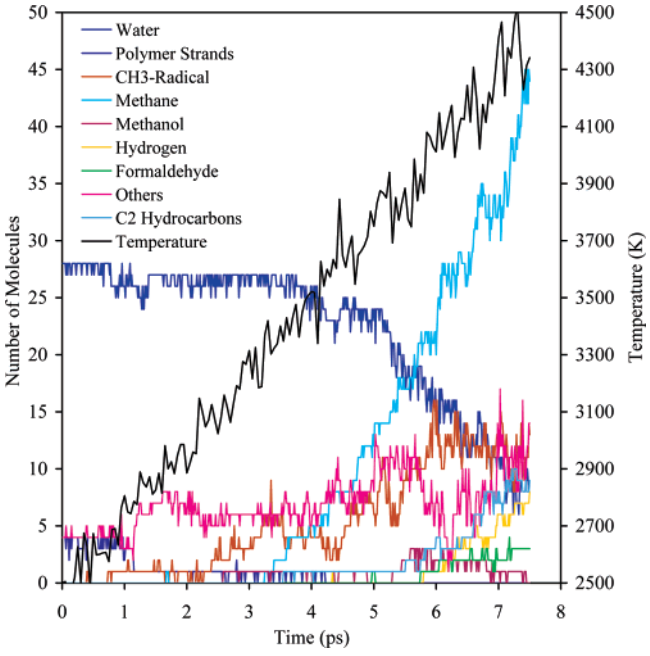


***Figure 14.*** Time evolution of the products from the cookoff simulation of PDMS with a 10% (w/w) water content.

17), at which temperature the ozone molecules begin to oxidize the polymer strands. This is in agreement with experimental work that has found that the presence of oxidizing agents accelerates the degradation process.[8−10] We observe the production of $CH_3O$ radical species after 3.5 ps that undergo a secondary reaction to form formaldehyde during the simulation.

The results from the cookoff simulations performed on the PDMS polymer in contact with NO are shown in Figure 18. Initial degradation of the polymer occurs at a slightly lower temperature of 2700 K in comparison to that of pure PDMS. Although homolytic Si−C bond cleavage initiates the degradation process, there was virtually no methane or other hydrocarbons formed during the simulation until the NO was consumed. This is in excellent agreement with experimental observations by Manders and Bellama[12] that showed that there

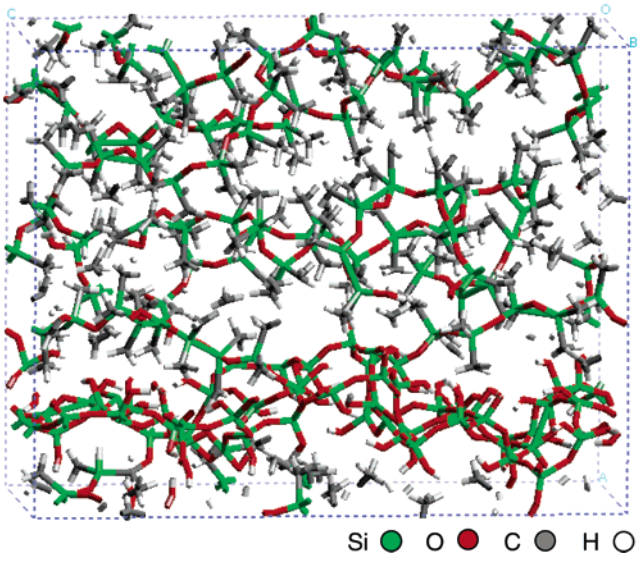


***Figure 15.*** Equilibrated configuration of PDMS in contact with a $SiO_2$ slab.

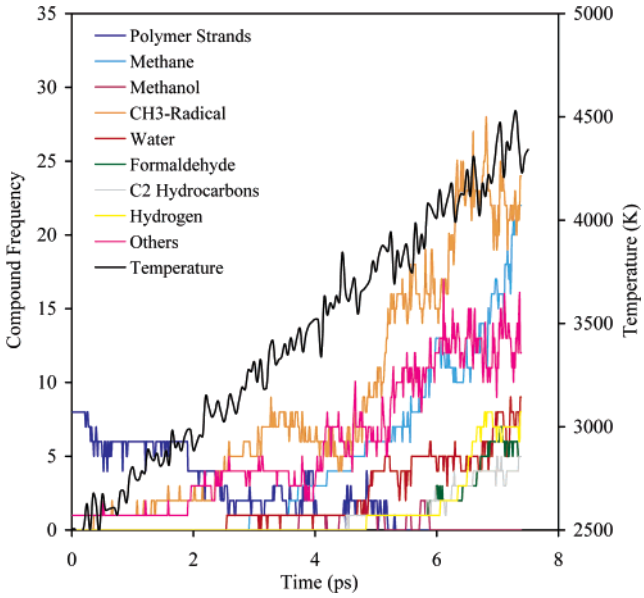


***Figure 16.*** Time evolution of the products from the cookoff simulation of PDMS in contact with an amorphous $SiO_2$ slab.

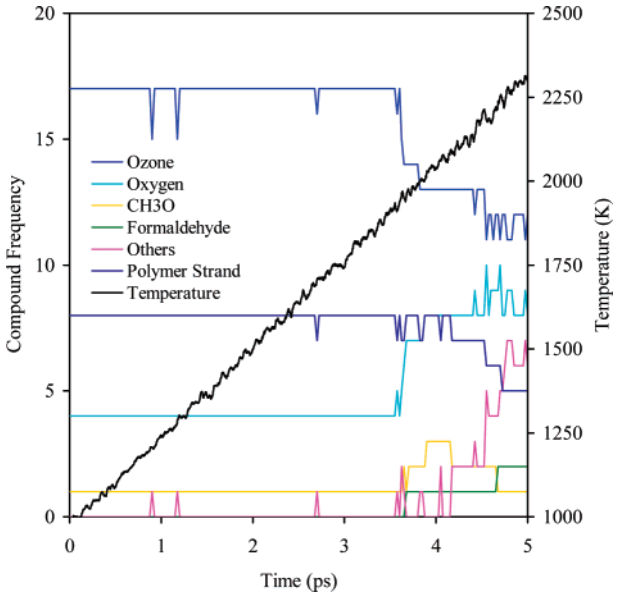


***Figure 17.*** Time evolution of the products from the cookoff simulation of PDMS in contact with 20 ozone molecules.

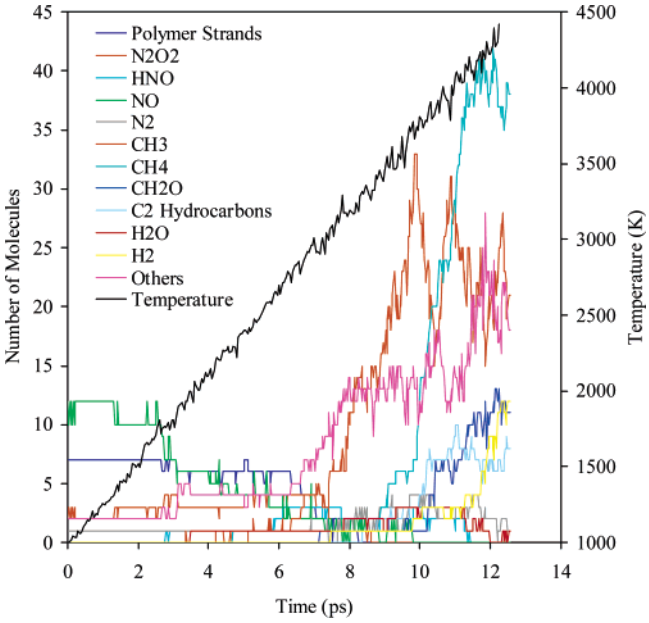


***Figure 18.*** Time evolution of the products from the cookoff simulation of PDMS in contact with 20 NO molecules.

were no hydrocarbon products from the experimental decomposition of 1 Torr of HMDS in the presence of 5 Torr of NO, thus validating that radicals were involved in the degradation process, as NO is known to be a free radical scavenger. During the initial degradation of PDMS, the NO reacts with the polymer radical species forming Si−N bonds and with the methyl radicals to produce formamide. After depletion of NO, the remainder of the products formed in the simulation is consistent with the results from the cookoff simulation of pure PDMS.

## Conclusion

By adding a suite of QM data to the ReaxFF $Si/SiO_2$ training set describing Si−C single and double bond, distortion of Si- and C-containing valence angles, structures, and relative energies relevant to PDMS chemistry, we have generated a ReaxFF description suitable for describing the decomposition of the PDMS polymer. We employed this force field to study the influence of temperature and pressure on PDMS stability. We found that, at heating rates of 266 K/ps, onset of PDMS degradation is observed at ∼2800 K. The decomposition is initiated by homolytic Si−C bond cleavage forming $CH_3$ radical species, which predominantly undergo a fast secondary reaction to form methane, which is the primary degradation product. On the basis of the rate of production of methane as a function of temperature, the energy of activation for PDMS decomposition was determined to be 53 kcal/mol. Our simulations of PDMS at various pressures indicate that the polymer stability increases with pressure, as the production of methane gets suppressed.

In addition to studying PDMS stability at various temperatures and pressures, we also investigated the impact of several additives on PDMS stability. We found that addition of 10% (w/w) water or an HO-terminated $SiO_2$ slab to the PDMS polymer does not significantly alter its decomposition temper-

ature, although these additions do have significant effects on the nature of the decomposition products. In the PDMS with 10% (w/w) water content, there were small polymer fragments produced and less cross-linking observed compared to that of the PDMS polymer. Addition of more reactive species, like ozone, leads to a significant drop in the PDMS decomposition temperature; in the presence of ozone the first decomposition reaction is observed at $T = 2000$ K. The onset temperature for degradation was only slightly reduced to 2700 K by the addition of NO. The NO reacted with the polymer and methyl radicals formed during the initial degradation of PDMS, and the production of hydrocarbons was only observed after the NO was completely consumed.

ReaxFF has provided useful insight into the high-temperature thermal properties of PDMS. All of our results are in good agreement with the available experimental observations, thus validating the role ReaxFF can play in elucidating the decomposition details of polymer materials.

**Acknowledgment.** We thank Los Alamos National Laboratory (LA-UR-04-8444) for providing partial funding for this project. The computational facilities of the MSC are also supported by grants from ARO-DURIP, ONR-DURIP, NSF-MRI, and the Beckman Institute. This work was also partially supported by DOE-ASC-Caltech.

**Supporting Information Available:** ReaxFF force field parameter data, figure showing comparison of ReaxFF and QC energies for Si−C single bond in $H_3Si-CH_3$, and figure showing ReaxFF and QC distortion energies. This material is available free of charge via the Internet at http://pubs.acs.org.

JA050980T